Available online at www.sciencedirect.com
ScienceDirect
International Journal of Solids and Structures 44 (2007) 34–50
INTERNATIONAL JOURNAL OF SOLIDS and STRUCTURES
www.elsevier.com/locate/ijsolstr

Orientation evolution in Hadfield steel single crystals under combined slip and twinning

D. Canadinc [a,*], H. Sehitoglu [a], H.J. Maier [b], D. Niklasch [b], Y.I. Chumlyakov [c]

[a] University of Illinois at Urbana-Champaign, Department of Mechanical and Industrial Engineering, 1206 W. Green St., Urbana, IL 61801, USA
[b] University of Paderborn, Lehrstuhl f. Werkstoffkunde (Materials Science), D-33095 Paderborn, Germany
[c] Siberian Physical–Technical Institute, Novosobornay Sq. 1, Tomsk, 634050, Russia

Received 12 December 2005; received in revised form 20 March 2006
Available online 22 April 2006

Abstract

The tensile deformation response and texture evolution of aluminum alloyed Hadfield steel single crystals oriented in the ⟨1 6 9⟩ direction is investigated. In this material, the strain hardening response is governed by the high-density dislocation walls (HDDWs) that interact with glide dislocations. A microstructure-based visco-plastic self-consistent model was modified to account for mechanical twinning in addition to the prevailing contribution of the HDDWs. Simulations revealed the contribution of twinning to the overall work hardening at the later stages of deformation. Moreover, both the deformation response and the rotation of the loading axis associated with plastic flow are successfully predicted even at the high-strain levels attained (0.53). Predicting the texture evolution serves as a separate check for validating the model, motivating its utilization in single and polycrystals of other alloys that exhibit combined HDDWs and twinning.

Keywords: Hadfield steel; Strain hardening; Crystal plasticity; Texture evolution; Dislocation walls

1. Motivation and significance

In a recent study investigating the strain hardening response of aluminum alloyed Hadfield steel (HSwAl), we attributed the unusually high-strain hardening coefficients ($\approx G/23$[1]) observed in the single crystals of this alloy to the formation of high-density dislocation walls (HDDWs) (Canadinc et al., 2005). Aluminum was added to Hadfield steel at 2.58 wt%, which normally has a chemical composition of 13.93 wt% Mn, 1.30 wt% C and balance Fe. The resulting material (HSwAl) with a face-centered cubic (fcc) structure at room temperature displayed HDDWs that form and evolve as a result of plastic deformation. The interaction

* Corresponding author. Present address: University of Paderborn, Lehrstuhl f. Werkstoffkunde (Materials Science), D-33095 Paderborn, Germany. Tel.: +49 5251 60 4228; fax: +49 5251 60 3854.
E-mail address: demircan.canadinc@gmail.com (D. Canadinc).

[1] G: the shear modulus.

0020-7683/$ - see front matter © 2006 Elsevier Ltd. All rights reserved.
doi:10.1016/j.ijsolstr.2006.04.011

between the HDDWs and active slip systems was shown to lead to the blockage of the glide dislocations by HDDWs, and eventually to the high-strain hardening rates under tensile loading. In this alloy, the strain hardening behavior is governed by HDDWs in multi-slip orientations ($\langle 1\,1\,1\rangle$ and $\langle 0\,0\,1\rangle$). However, twinning is also present as a secondary deformation mechanism in the single-slip orientation $\langle 1\,2\,3\rangle$, although the volume fraction is much less than that of HDDWs (Canadinc et al., 2005). A microstructure-based model was proposed, that successfully predicts the tensile deformation response of HSwAl single crystals (Canadinc et al., 2005). The appeal of the model lies in the simplicity of the constitutive relationship that successfully captures the role of HDDWs and twinning (where prevalent) on the overall deformation response of the material.

Previously, the HDDWs had been observed by several researchers to be effective in materials of both face-centered cubic (fcc) and body-centered cubic (bcc) structures (Winther et al., 1997; Winther, 1998; Hansen and Juul Jensen, 1992; Juul Jensen and Hansen, 1990; Peeters et al., 2000, 2001; Raphanel et al., 1992; Liu and Hansen, 1995; Liu et al., 1998). These studies revealed the existence of HDDWs and their influence on the overall deformation response through detailed transmission electron microscopy (TEM) studies. The HDDWs have been shown to interact with dislocations that carry the plastic deformation on the active slip systems, resulting in an overall hardening: glide dislocations get trapped at the boundaries of the HDDWs, and thus the dislocation motion is blocked on an active slip system interacting with a HDDW. In our recent study on single crystals of HSwAl (Canadinc et al., 2005), we obtained results that very well agreed with these previous observations.

Contrary to many of the previous contributions that investigated the HDDWs in pure metals and alloys (Winther et al., 1997; Winther, 1998; Hansen and Juul Jensen, 1992; Juul Jensen and Hansen, 1990; Peeters et al., 2000, 2001; Winther, 1998; Raphanel et al., 1992; Liu and Hansen, 1995; Liu et al., 1998), we utilized single crystals (Canadinc et al., 2005) to study the HDDWs. This eliminated the complications resulting from grain boundary effects and interactions between neighboring grains. We established a model that supports our explanation of how the HDDWs contribute to the overall hardening by successfully predicting the material's response to applied loading for several crystallographic orientations: $\langle 1\,1\,1\rangle$, $\langle 0\,0\,1\rangle$, and $\langle 1\,2\,3\rangle$. The key finding is that the volume fraction of HDDWs evolves with deformation leading to very high-strain hardening coefficients in this material.

Prior to our work on the strain hardening response of HSwAl (Canadinc et al., 2005), the unusual strain hardening response of Hadfield steel was linked to various causes, including the formation of twin boundaries that provided strong barriers to dislocation motion (Adler et al., 1986; Karaman et al., 2000a,b, 2001a,b,c). Interruption of the glide dislocation path by stacking faults (Shtremel and Kovalenko, 1987) has also been forwarded to explain the unusual strain hardening of the Hadfield steel. In addition, several researchers suggested that dynamic strain aging is the mechanism underlying the rapid strain hardening exhibited by Hadfield steel (Dastur and Leslie, 1981; Owen and Grujicic, 1999). Among these proposed mechanisms, twinning has been the most prevalent one to explain the unusual strain hardening of Hadfield steel. In order to investigate the role of slip on this unusual strain hardening in detail, we introduced aluminum to the microstructure of Hadfield steel (Canadinc et al., 2005). It has been shown that in low stacking fault energy alloys, intrinsic stacking faults serve as precursors to twinning, such that intrinsic stacking faults observed at the very early stages of deformation thicken into twin lamellae with further plastic deformation (Raghavan et al., 1969). Therefore, aluminum was added to the microstructure of Hadfield steel in order to increase the stacking fault energy and thereby suppress twinning, by preventing the formation of intrinsic stacking faults at small strains and their further growth into twin lamellae. Alloying Hadfield steel with aluminum suppressed twinning in multi-slip orientations or limited its occurrence to very low volume fractions (less than 5%) even at very high-plastic strains (more than 0.25) (Canadinc et al., 2005).

In the work presented herein, the focus is on validating the microstructure-based model by applying it to single crystals of other crystallographic orientations. Moreover, the texture evolution (rotation of the loading axis) is utilized as a separate tool for checking the validity of the model. Specifically, the experimentally measured textures were compared to the simulation results at various strains along the deformation. In addition, the role of twinning on the strain hardening response of a single-slip orientation single crystal was also investigated, in order to establish the contribution of twinning to the overall hardening in the presence of HDDWs.

The current work focuses on the texture evolution in the presence of HDDWs. The previous studies on HDDWs considered the texture evolution (Winther et al., 1997; Hansen and Juul Jensen, 1992; Juul Jensen

and Hansen, 1990; Peeters et al., 2000, 2001); however, these investigations were mostly limited to polycrystalline materials. The evolution of texture in the presence of HDDWs that form by mutual trapping of glide dislocations was laid out on a statistical basis with the aid of computer simulations (Winther, 1998; Raphanel et al., 1992; Liu and Hansen, 1995; Liu et al., 1998). Extended Taylor algorithms were utilized to establish the increase in flow stress due to HDDWs and monitor the corresponding changes in texture. Nevertheless, no results have been forwarded linking the macroscopic deformation response and the corresponding texture evolution in the presence of HDDWs, warranting further investigation of texture evolution in alloys exhibiting HDDWs.

The interaction of HDDWs with glide dislocations moving on the active slip systems and the evolution of the volume fraction of HDDWs during plastic deformation (Canadinc et al., 2005) constitutes a highly anisotropic phenomenon (Canadinc et al., submitted for publication). Considering the orientations which exhibit deformation beyond plastic strains of 0.20 (e.g., $\langle 0\,0\,1\rangle$ and $\langle 1\,2\,3\rangle$ orientations), the influence of these anisotropic structures on the texture evolution is inevitable. With this motivation, we undertook the present study in order to investigate the texture evolution in the presence of HDDWs in detail. Specifically, we examined the rotation of the loading axis due to plastic deformation of single crystals of HSwAl in the presence of HDDWs. Utilization of single crystals eliminates complications brought about by the presence of multiple grains, and promotes a more clear understanding of the texture evolution in this class of alloys.

In the present work, we examined the room temperature deformation response of HSwAl single crystals loaded in the $\langle 1\,6\,9\rangle$ direction. In addition to the prediction of the macroscopic deformation response, we utilize the texture evolution as a tool for validating our model (Canadinc et al., 2005) that incorporates the HDDWs into a visco-plastic self-consistent (VPSC) algorithm. Furthermore, we report the role of mechanical twinning on the strain hardening response of Hadfield steel in the presence of HDDWs. Overall, our combined experimental and modeling effort reported here provides a venue for extending the application of our model to other crystallographic orientations, and polycrystals of various alloys and metals that exhibit HDDWs.

2. Background

2.1. HDDWs: formation, evolution and interaction with slip systems

In our previous work (Canadinc et al., 2005), we investigated the formation and evolution of HDDWs through a detailed TEM study. Single crystals of several orientations ($\langle 1\,1\,1\rangle$, $\langle 0\,0\,1\rangle$, and $\langle 1\,2\,3\rangle$) were examined with TEM at various stages of deformation in order to shed light onto the role of HDDWs on the rapid strain hardening exhibited by HSwAl. The HDDWs, present at all stages of deformation in the single crystals of HSwAl (Fig. 1), reside predominantly on the $\{1\,1\,1\}$ planes in the fcc materials. The volume fraction of HDDWs increases through the mutual trapping of glide dislocations due to the interaction of HDDWs with the active slip systems (Fig. 2), as the deformation progresses. The dislocation density of the HDDWs is very high at the final stages of deformation, prior to fracture (Fig. 1(b)).

The interaction of HDDWs with the active slip systems, as illustrated in Fig. 2, takes place when the HDDWs block the glide of dislocations on an active slip system (Canadinc et al., 2005, submitted for publication). As plastic deformation progresses, a set of HDDWs that reside on the active slip system q (with the plane normal N_q) forms, and the HDDWs evolve with increasing strain. An HDDW may intersect the path of dislocations moving on the plane of another active slip system n (with the plane normal N_n) in the direction as specified by the burgers vector b_n. This results in the trapping of the dislocations on the slip system n in the HDDWs. The angle θ_{nq} between the vectors b_n and N_q constitutes a measure of this blockage of glide dislocations by HDDWs. When the HDDWs and the slip system n are coplanar the interference is minimized as manifested through the angle θ_{nq}.

The slip system–HDDW interaction takes place at the dislocation level, and we consider several mechanisms during these interactions. The HDDWs form on or parallel to the most active slip systems, and the mobile dislocations on these slip systems are expected to contribute to their dislocation density. Based on TEM observations at small strains prior to the well-development of HDDWs (Canadinc et al., 2005), formation of dislocation pile-ups is proposed to be the primary mechanism for mobile dislocations to get trapped in the HDDWs forming "on" the very plane of an active slip system. If the HDDWs form on a plane "parallel"

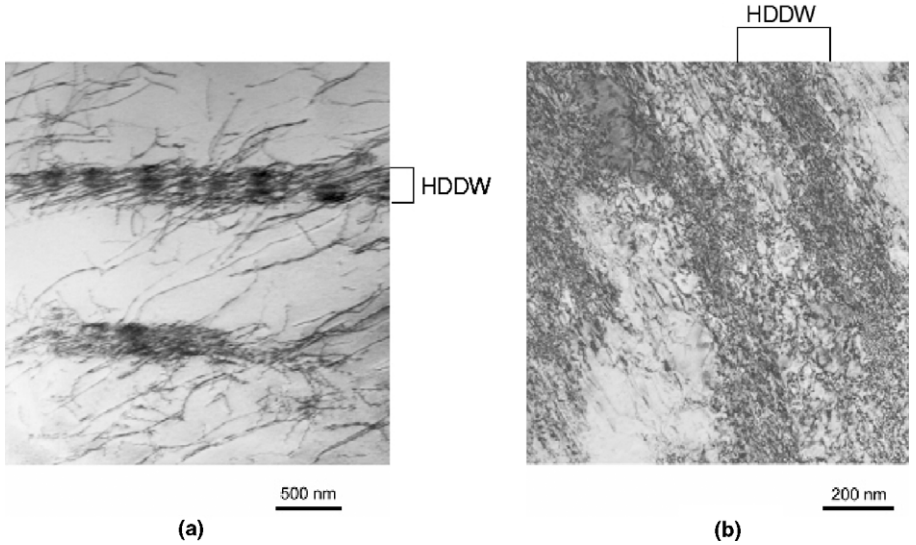

Fig. 1. TEM images showing the HDDWs and localized dislocation activities in single crystals under monotonic tensile loading. (a) HSwAl ⟨1 2 3⟩ orientation at 3% strain: early stages of HDDW formation. (b) HSwAl ⟨1 2 3⟩ orientation at 62% strain: the local density of dislocations trapped in the HDDWs becomes higher at larger strains. The ⟨1 2 3⟩ orientation is very close to the ⟨1 6 9⟩ orientation investigated in this paper, and has very similar material properties.

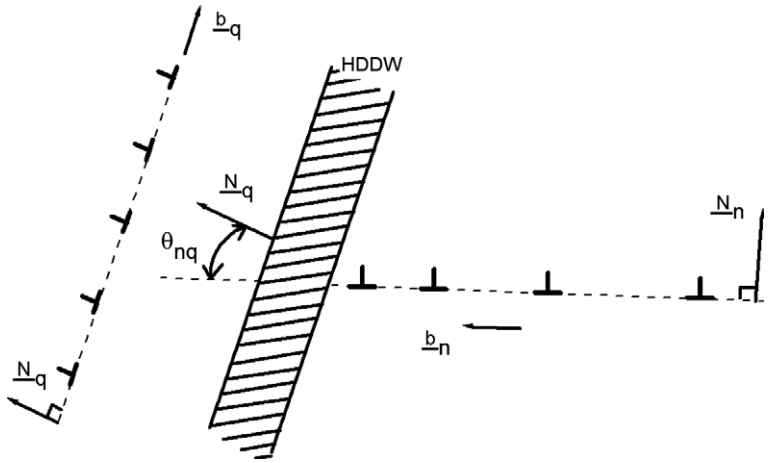

Fig. 2. A schematic showing the interaction between a HDDW, that formed parallel to the plane of the active slip system (q), and another active slip system (n) within a single crystal (or grain).

to the active slip system, then the contribution is achieved by double cross slip (Fig. 3(a)), such that the mobile screw dislocations reach the HDDWs parallel to their slip plane and become immobilized (Peeters et al., 2001). Annihilation of mobile dislocations with immobile dislocations can take place through the disintegration of edge dislocations of opposite signs.

The interaction of HDDWs with mobile dislocations of a conjugate slip system is proposed to take place in the following way: in most metals, dislocations dissociate into two Shockley partials in their own slip systems. If the dislocations on two {1 1 1} planes meet at an intersection, depending on the particular directions of the Burgers vectors of the leading partials, there is a repulsive or attractive force between these partials (Hull and Bacon, 2002). Similarly, if a dislocation on a {1 1 1} plane meets with another dislocation trapped at a HDDW, there is either repulsion or an attraction between the two leading partials. If the two leading partials combine

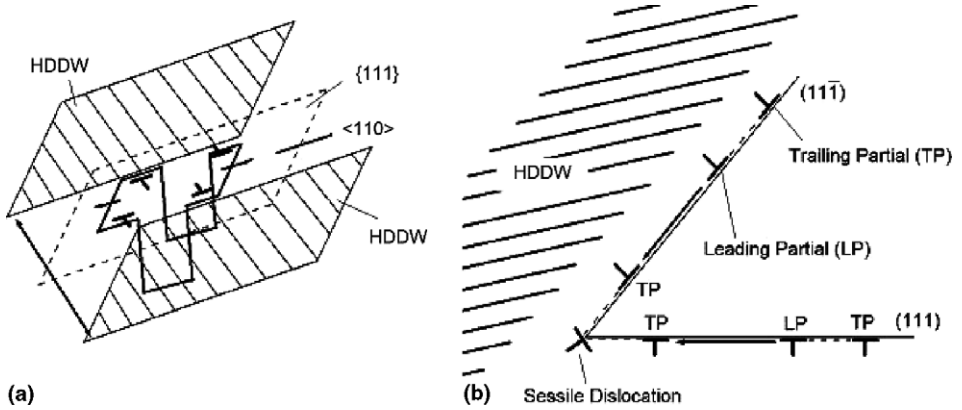

Fig. 3. Evolution of HDDWs due to (a) double cross slip (after Peeters et al., 2001) and, (b) HDDW–slip system interaction (after Weertman and Weertman, 1992).

at the intersection, the combination is a sessile dislocation, and exerts a repulsive force on the trailing partials, forming a stable arrangement (Fig. 3(b)). Due to this sessile arrangement, further dislocation glide is prevented on both {1 1 1} planes, leading to more pile-ups around the boundary of the HDDWs (Fig. 2), further increasing the density of dislocations trapped at the HDDWs. As the plastic deformation progresses, more dislocations get trapped at HDDWs due to their increasing strength as a barrier to dislocation glide. Further details of the formation and evolution of HDDWs could be found in Peeters et al. (2001).

2.2. Texture evolution

It has not yet been fully understood how the formation and evolution of HDDWs, and their interaction with active slip systems influence the texture evolution. This alone warrants a closer look at the texture evolution of HSwAl single crystals for an improved understanding of the influence of HDDWs. Moreover, texture is an important "element" of the microstructure. As we try to understand the unusual strain hardening

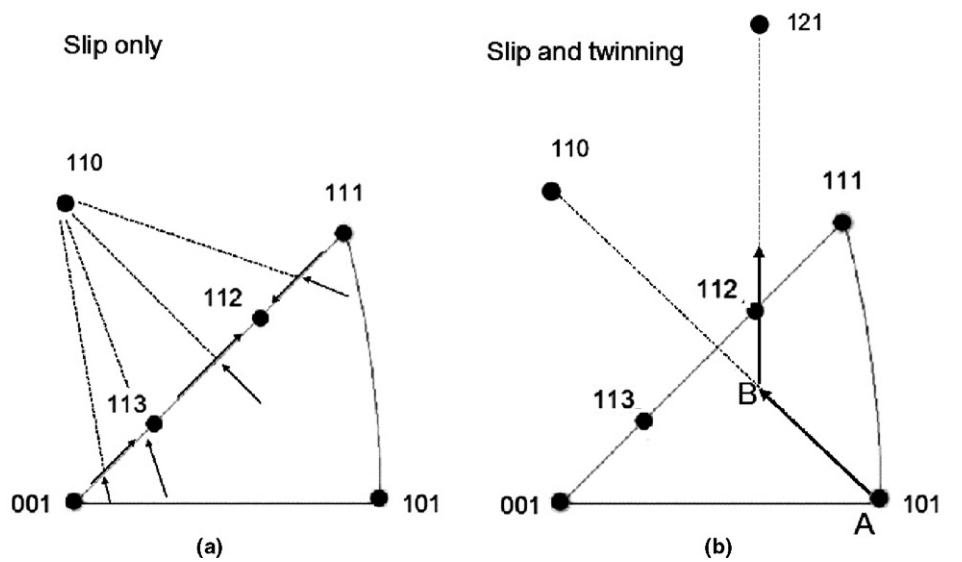

Fig. 4. Schematic showing the texture evolution in fcc materials (a) with slip as the deformation mechanism only (after Hosford, 1993), and (b) with slip and twinning. The stereographic triangle shown represents the smallest symmetry element of a stereographic projection for a cubic crystal.

behavior of Hadfield steels utilizing a microstructure-based model, a thorough investigation of texture evolution in this material is necessary.

When the deformation occurs by dislocation glide only, for an fcc crystal oriented with the tensile axis inside the primary stereographic triangle, the tensile axis rotates toward the [1 1 0] direction, until it reaches the (0 0 1)–(1 1 1) boundary. Along this boundary, the primary and conjugate systems are equally favored. Afterwards, simultaneous [1 0 1] and [1 1 0] slip causes rotation toward the [1 1 2] orientation (Fig. 4(a)) (Hosford, 1993). However, in the case of overshooting, the rotation continues toward the [1 1 0] orientation after the tensile axis reaches the (0 0 1)–(1 1 1) boundary.

If twinning is activated at any point along the deformation, the rotation of the tensile axis deviates from its path towards the [1 1 0] orientation, and is redirected toward the [1 2 1] orientation (Fig. 4(b)) (Zakharova et al., 2002). Fig. 4(b) illustrates a hypothetical case where an fcc crystal starts deforming through the $\langle 1\,1\,0\rangle(1\,1\,1)$ primary slip at point A. Here, the hypothetical initial orientation at 'A' corresponds to the [1 0 1] orientation. As the plastic deformation progresses, the loading axis of the crystal rotates toward the [1 1 0] orientation. The activation of mechanical twinning of the $\langle 1\,1\,2\rangle\{1\,1\,1\}$ family takes place at point 'B', and the rotation of the axis is directed towards the [1 2 1] orientation, as shown.

3. Modeling the deformation response under combined slip and twinning

In order to improve the understanding of the strain hardening behavior of Hadfield steels further, we proposed a model that takes into account experimental data regarding the formation and evolution of HDDWs (Canadinc et al., 2005, submitted for publication). The microstructure-based model utilizes a crystal plasticity description of the strain rate at the single crystal level, and the reference stress evolves with the dislocation density. The HDDW–slip system interaction is incorporated into the overall rate of dislocation density ($\dot{\rho}$) in the following format:

$$\dot{\rho} = \sum_n \{k_1\sqrt{\rho} - k_2\rho\}|\dot{\gamma}^n| + \sum_n \sum_q \frac{K}{db}\cos\theta_{nq}|\dot{\gamma}^n| \tag{1}$$

where k_1 and k_2 are constants, K is a geometric constant (Canadinc et al., 2003, 2005, submitted for publication), and b stands for (the magnitude of) the burgers vector. The first term $\sum_n\{k_1\sqrt{\rho} - k_2\rho\}|\dot{\gamma}^n|$ represents the athermal (statistical) storage of moving dislocations ($k_1\sqrt{\rho}$) and dynamic recovery ($-k_2\rho$) in the domains outside the HDDWs (Canadinc et al., 2003), whereas the second term $\sum_n\sum_q \frac{K}{db}\cos\theta_{nq}|\dot{\gamma}^n|$ accounts for the contribution due to HDDWs formed parallel to the plane of the slip system q acting as effective obstacles to the moving of dislocations gliding on the active slip system n (Fig. 2). In other words, the second term represents an empirical geometric storage of dislocations due to HDDWs, which subdivide the matrix domains and thereby decrease the mean free path of dislocations (Canadinc et al., 2003). The angle θ_{nq} is the angle between the direction of slip in the active slip system n and the normal to the plane of the slip system q, and is incorporated as a measure of the interaction between HDDWs and glide dislocations in a geometric sense. Thus, the angle θ_{nq} is a variable, such that it can take different values depending on the active slip systems and the HDDWs they interact with. Moreover, the θ_{nq} continues to change as the deformation progresses, due to the rotation of HDDWs in the matrix. The term d represents the average spacing between the dislocation sheets. The term $\dot{\gamma}^n$ stands for the rate of shear in the active slip system n.

By only accounting for the change in the overall rate of dislocation density (Eq. (1)), the model falls short of accounting for the rapid strain hardening of the HSwAl. The HDDWs are treated as impenetrable barriers to dislocation motion, acting as hard phases in the matrix, similar to precipitates. Accordingly, HDDWs are modeled as (elongated) ellipsoidal inclusions in the matrix. As plastic strain progresses, Orowan loops are stored around the HDDWs, giving rise to long-range internal stresses in the matrix (Canadinc et al., 2003). This additional hardening (τ^B) due to HDDWs acting as hard phases in the matrix is included through the term:

$$\tau^B = 2f\xi\mu\sum_n |\gamma^n| \tag{2}$$

where the terms μ, ξ, and f stand for the shear modulus, the Eshelby accommodation factor (elongated ellipsoidal inclusions) (Brown and Clarke, 1975), and the volume fraction of HDDWs, respectively. The $\sum_n|\gamma^{(n)}|$

term is simply the summation of the magnitudes of the shear strains on the active slip systems and represents the total matrix mismatch strain brought about by the high-density dislocation sheets. The volume fraction of HDDWs (f) is a variable, and accounts for the evolution of HDDWs with increasing plastic deformation. As the plastic deformation progresses, more glide dislocations are trapped at their boundaries, adding to the overall volume fraction of HDDWs (Canadinc et al., 2005).

Following the incorporation of the additional hardening terms due to the HDDWs, the original rate of flow stress $\dot{\tau}$ defined in the traditional Taylor hardening format as

$$\dot{\tau} = \frac{\alpha \mu b \dot{\rho}}{2\sqrt{\rho}} \tag{3}$$

becomes

$$\dot{\tau} = \sum_n \left[\frac{\alpha^2 \mu^2 bK}{4t(\tau - \tau_0)} \frac{f}{1-f} \sum_q \cos\theta_{nq} + 2f\xi\mu + \left\{ \theta_0 \left(\frac{\tau_s - \tau}{\tau_s - \tau_0} \right) \right\} \right] |\dot{\gamma}^n| \tag{4}$$

where $\left\{ \theta_0 \left(\frac{\tau_s - \tau}{\tau_s - \tau_0} \right) \right\}$ is the well-known Voce hardening term, with τ_0 as the reference strength, and θ_0 and τ_0 as the parameters that define the hardening. The term α is the dislocation interaction parameter (Saada, 1960; Venables, 1963).

The solution of the stresses and strains, on the other hand, is accomplished by implementing the model outlined in Eqs. (1)–(4) into the visco-plastic self-consistent (VPSC) algorithm originally developed by Tome and Lebensohn (Lebensohn and Tomé, 1993). The VPSC solves for stresses and strain as explained in the following: plastic deformation occurs when a slip or a twinning system becomes active. The resolved shear stress, τ^s_{RSS}, for a system (s) is given by

$$\tau^s_{\mathrm{RSS}} = m^s_i \sigma_i \tag{5}$$

where m^s_i is the vector form of the Schmid tensor and σ_i is the vector form of the applied stress. To describe the shear rate in the system, s, a non linear shear strain rate as a power of τ^s_{RSS} is written as

$$\dot{\gamma}^s = \dot{\gamma}_0 \left(\frac{\tau^s_{\mathrm{RSS}}}{\tau^s_0} \right)^n = \dot{\gamma}_0 \left(\frac{m^s_i \sigma_i}{\tau^s_0} \right)^n \tag{6}$$

where $\dot{\gamma}_0$ is a reference rate, τ^s_0 is the threshold stress corresponding to this reference rate, and n is the inverse of the rate sensitivity index. If n is high enough, this description asymptotically approaches the rate insensitive limit. The total strain rate in a crystal can be written as the sum of all potentially active systems and can be pseudolinearized as follows (Lebensohn and Tomé, 1993):

$$\dot{\varepsilon}_i = \left[\dot{\gamma}_0 \sum_1^s \frac{m^s_i m^s_j}{\tau^s_0} \left(\frac{m^s_k \sigma_k}{\tau^s_0} \right)^{n-1} \right] \sigma_j = M^{c(\mathrm{sec})}_{ij}(\tilde{\sigma}) \sigma_j \tag{7}$$

where $M^{c(\mathrm{sec})}_{ij}$ is the secant visco-plastic compliance of the crystal which gives the instantaneous relation between stress and strain rate.

Following Lebensohn and Tomé (1993), at the polycrystal level the same pseudolinear form can be implemented as in the case of Eq. (7) as follows:

$$\dot{E}_i = M^{(\mathrm{sec})}_{ij}(\tilde{\Sigma}) \Sigma_j + \dot{\Sigma}^0 \tag{8}$$

where $\dot{E}_i$ and Σ are the polycrystal strain rate and applied stress.

Defining the deviations in strain rate and stress between the local (single crystal level) and the overall (polycrystalline) magnitudes as

$$\tilde{\dot{\varepsilon}}_k = \dot{\varepsilon}_k - \dot{E}_k \tag{9}$$

$$\tilde{\sigma}_j = \sigma_j - \Sigma_j \tag{10}$$

where $\dot{\varepsilon}_k$ and σ_j stand for the local (single crystal or grain level) strain rate and stress. Utilizing Eshelby's inhomogeneous inclusion formulation one can solve the stress equilibrium equation to derive the following interaction equation (Kocks et al., 2000)

$$\tilde{\dot{\varepsilon}} = -\widetilde{M} : \tilde{\sigma} \tag{11}$$

The interaction tensor $\widetilde{M}$ is defined as

$$\widetilde{M} = n'(I - S)^{-1} : S : M^{(\mathrm{sec})} \tag{12}$$

where $M^{(\mathrm{sec})}$ is the secant compliance tensor for the polycrystal aggregate and S is the visco-plastic Eshelby tensor (Kocks et al., 2000).

In this formulation, the visco-plastic moduli of the grain and the homogeneous medium are assumed to be known in advance, which is not the case. Therefore a self-consistent expression must be found from which the macroscopic secant compliance, $M^{(\mathrm{sec})}$, can be determined by substituting Eqs. (7) and (8) in Eq. (11). The macroscopic strain rate is evaluated by taking the weighted average of crystal strain rates over all the crystals as follows:

$$M^{(\mathrm{sec})} = \langle M^{\mathrm{c}(\mathrm{sec})} : (M^{\mathrm{c}(\mathrm{sec})} + \widetilde{M})^{-1} : (M^{(\mathrm{sec})} + \widetilde{M}) \rangle \tag{13}$$

Iterative solution of Eqs. (7), (11) and (13) gives the stress in each crystal, the crystal's compliance tensor, and the polycrystal compliance consistent with the applied strain rate $\dot{E}_i$. In this work, we chose the term n (in Eq. (6)) to be in the rate insensitive limit ($n = 20$). As for the interaction equation (12), an effective value of $n' = 1$ is used.

The present model considers a polycrystalline aggregate and an initial texture information in the form of spatial orientations of the grains in this aggregate. This information is supplied as an input, which consists of three sets of Euler angles. In the simulation of single crystals, we considered the single crystals as polycrystalline aggregates (Canadinc et al., 2003, 2005; Karaman et al., 2000a,b, 2001a,b,c) consisting of grains all of which have the same initial orientation in the Eulerian space. A few grains (randomly selected but not neighboring) are intentionally misoriented with a slight deviation from the original orientation for the sake of numerical conversion. The Euler angles for each single crystal orientation were determined (Bunge, 1969) at the stage of single crystal growth and the cutting of different orientations out of these crystals.

The self-consistent algorithm is solved with three nested iterations (Canadinc et al., 2005): the outer iteration varies the stress and the compliance in each grain. The intermediate iteration varies the overall tangent modulus of the aggregate (Turner et al., 1999), whereas the inner iteration varies the overall secant compliance.

The novelty of the modeling effort presented herein lies in the tackling of the problem of implementing the evolution of the HDDWs and their contribution to the hardening of the material. The original VPSC algorithm does not account for such structures and their influence on the deformation behavior.

In previous studies (Canadinc et al., 2003; Karaman et al., 2000a,b, 2001a,b,c), we successfully modeled the slip–twin interactions using the capabilities of VPSC. A unique hardening formulation was proposed in the constitutive model incorporating length scales (based on TEM observations) associated with spacing between twin lamellae and grain boundaries (Karaman et al., 2000a,b, 2001a,b,c). Many of the experimental findings were made on $\langle 1\,1\,1 \rangle$ and $\langle 1\,4\,4 \rangle$ crystallographic orientations deformed in tension, displaying fine twin lamellae at small strains in addition to slip in intra-twin regions. A natural outcome of the model was the small deformation activity inside the twinned regions and higher deformations between the twins. In addition, this VPSC model was modified to account for precipitation and twinning length scales in Hadfield steel with 1.06 wt.% nitrogen for selected crystallographic orientations (Canadinc et al., 2003). Incoherent precipitates in the hardening formulation were treated as factors affecting the mean free path of dislocations. The model also accounts for plastic relaxation of precipitates with increasing strain, and accurately predicts the stress–strain response.

In the present study, we utilized a similar procedure to account for HDDWs (and their contribution to hardening) as adopted in twinning and twin reorientation schemes. In a recent study (Canadinc et al., 2003), we demonstrated the influence of twinning on hardening as hard boundaries that constitute an obstacle to dislocation motion. Based on these previous observations and modeling efforts, we modeled the simultaneous evolution of

HDDWs and mechanical twins on characteristic slip and twin planes with their respective volume fraction evolution (Canadinc et al., 2005). The HDDWs act as hard phases (or boundaries) that block the dislocation motion, and part of these blocked dislocations become trapped and add to the density of HDDWs, fundamentally posing a similar barrier as twins with further straining (Fig. 2) (Canadinc et al., 2005).

In the first phase of this study (Canadinc et al., 2005), we introduced the conventional trace analysis results into the VPSC algorithm in the form of plane normals and directions associated with the possible (1 1 1) planes that HDDWs form on. As mentioned earlier, the HDDWs formed parallel to the planes of the most active slip systems, which was confirmed by trace analysis (Canadinc et al., 2005). Therefore VPSC was given the normals of the sets of HDDW planes. Slip directions and slip planes for fcc crystal were also provided. As the sample is strained, the HDDWs, which act as barriers to dislocation motion in the matrix, rotate similar to the rotation of lattice slip systems. This was accounted for in our simulations as large strains (0.10) were realized. Moreover, at each incremental step of the simulations, the volume fraction of HDDWs was modified, to reflect their evolution along with increasing strain (Canadinc et al., 2005). Our HDDW volume fraction evolution resemble that of the twin volume fraction in the VPSC, albeit with different hardness and lattice planes. Therefore, at each step, the HDDWs increased in their dislocation densities and underwent continuous reorientation, similar to the twin volume fraction evolution, which is explained in what follows.

Here, it is assumed that, similar to slip, twinning has associated a critical resolved shear of activation in the twinning plane and along the twinning direction (Lebensohn and Tomé, 1993), and therefore Eqs. (5)–(13) hold for both slip and twinning. However, this resolved shear stress differs from slip in its directionality, which is modeled by ascribing a very high-threshold stress in the opposite direction. Another important fact is that the twinned fractions possess a different orientation than the surrounding matrix. In addition to contributing to the texture, the twinned regions also act as effective barriers to dislocation motion and growth of other twin lamellae. The hardening induced by the twins is empirically enforced by assigning high values to the latent hardening coefficients describing the slip–twin and twin–twin interactions (Lebensohn and Tomé, 1993). The effect of twinning on the texture evolution is reflected by the volume fraction of the twinned regions: within each crystal, the shear strain γ^t contributed by each twin system t, is related to the associated volume fraction f^t and the characteristic twin shear S^t (0.707, following Karaman et al., 2000a,b, 2001a,b,c; Canadinc et al., 2003) as

$$f^t = \frac{\gamma^t}{S^t} \tag{14}$$

The sum over all twin systems represents the accumulated twin volume fraction in a single crystal (or grain):

$$f = \sum_t \frac{\gamma^t}{S^t} \tag{15}$$

Accordingly, the pseudolinearized form of the total strain rate (Eq. (7)) could also be written to reflect both slip (s) and the volume fraction of twinned (t) regions, such that

$$\dot{\varepsilon}_i = \left[(1-f)\dot{\gamma}_0 \sum_1^s \frac{m_i^s m_j^s}{\tau_0^s} \left(\frac{m_k^s \sigma_k}{\tau_0^s} \right)^{n-1} + f\dot{\gamma}_0 \sum_1^t \frac{m_i^t m_j^t}{\tau_0^t} \left(\frac{m_k^t \sigma_k}{\tau_0^t} \right)^{n-1} \right] \sigma_j = M_{ij}^{c(sec)}(\tilde{\sigma})\sigma_j \tag{16}$$

4. Experimental techniques

The material investigated in this study is aluminum alloyed Hadfield steel (HSwAl) with a chemical composition of 13.93 wt% Mn, 1.30 wt% C, 2.58 wt% Al and balance Fe. The crystal structure of this material at room temperature is face-centered cubic (fcc). The Bridgman technique was employed to grow single crystals on ⟨1 1 1⟩ seeds in magnesia crucibles in a He atmosphere. Homogenization of the single crystals was carried out at 1323 K for 20 h in a vacuum sealed furnace. Electro-discharge machining (EDM) was utilized to cut small-scale dog-bone shaped tension specimens with a gauge length of 10 mm. The samples were tested utilizing a hydraulic test frame equipped with a digital controller. A miniature extensometer with a gauge length of 3 mm was employed for accurate strain measurement in the gauge section. Samples were analyzed with

electron back scatter diffraction (EBSD) before and during deformation to monitor the texture evolution due to deformation. Specimens were deformed with certain strain increments, and texture was measured after each increment of deformation. The tests were run at a slow strain rate of $4 \cdot 10^{-4} \frac{1}{s}$. Finally, the room temperature tensile deformation response of titanium-stabilized interstitial free (IF) steel (Niendorf et al., submitted for publication) was also investigated in order to emphasize the role of HDDWs and twinning, by comparison of HSwAl and IF steel. The IF steel utilized in this study is a commercial grade ferritic steel as used in deep drawing applications. It has a very low carbon content, and possesses additional micro alloying elements, such as titanium and niobium, which bind the carbon to the grain boundaries in the form of carbides leading to grain interiors nearly free of interstitial atoms (Niendorf et al., submitted for publication).

5. Deformation response and accompanying texture evolution

The room temperature stress–strain response of HSwAl is reported in Fig. 5. We considered the ⟨1 6 9⟩ orientation under tensile loading. This particular crystallographic orientation was chosen based on the following reasons: first of all, according to our previous results on the single crystals of HSwAl (Canadinc et al., 2005), the ⟨1 2 3⟩ orientation exhibits the highest plastic strains (up to 0.62) under tensile loading. The ⟨1 6 9⟩ orientation, being close to the ⟨1 2 3⟩ orientation with a very similar Schmid factor, is expected to display a similar amount of ductility. Such ductility allows the texture evolution to be monitored in a relatively broader range of deformation compared to other orientations. Another reason is that, although being practically close to the

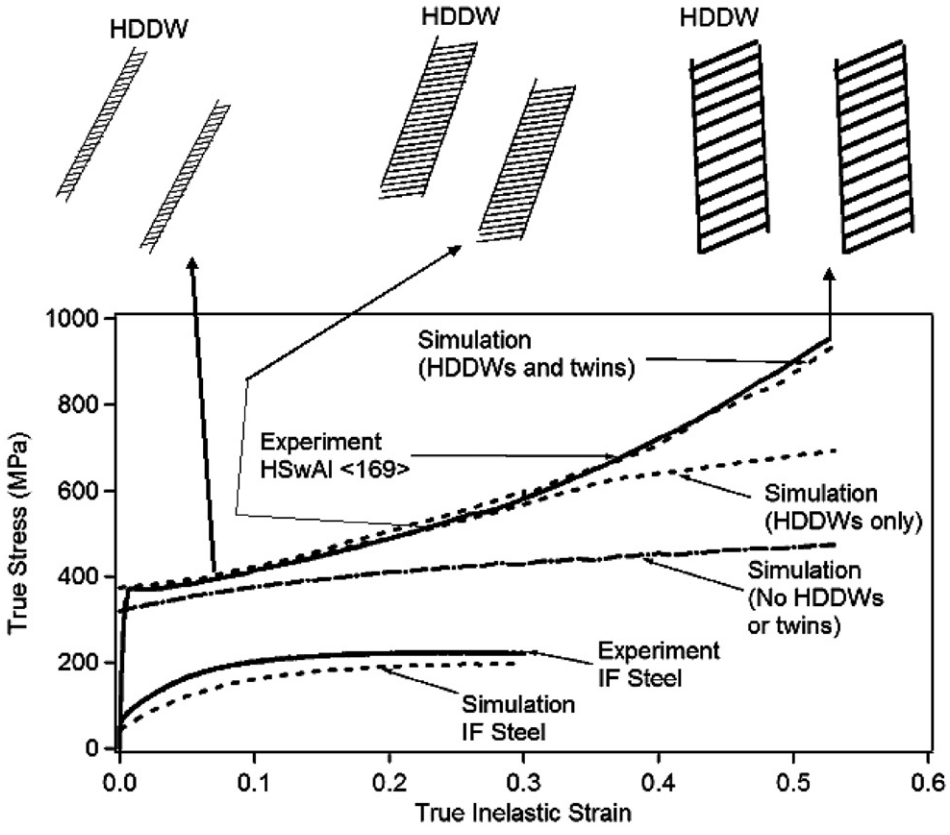

Fig. 5. Comparison of experiments and simulations of the room temperature tensile stress–strain behavior of the ⟨1 6 9⟩ orientation single crystals of HSwAl. The results of simulations accounting for twinning, and disregarding the role of HDDWs are also shown. The accompanying schematic describes the volume fraction evolution and rotation of HDDWs. Note that the amount of rotation and volume fraction evolution shown in the schematic do not represent experimental data. Experimental data for bcc IF steel polycrystals (Niendorf et al., submitted for publication) and the corresponding simulation results are also shown.

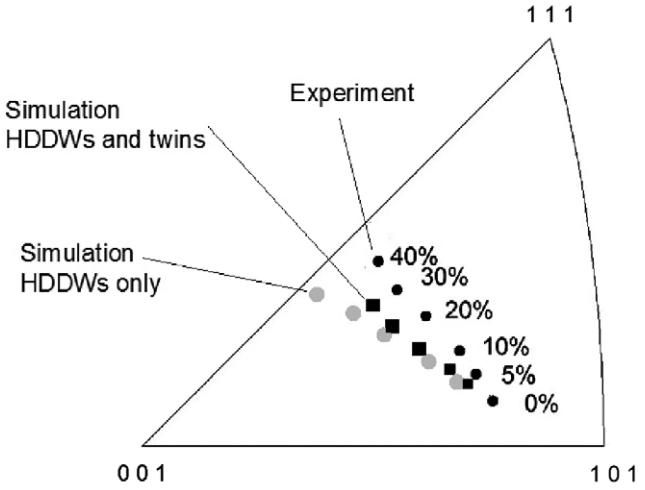

Fig. 6. Comparison of measured and calculated texture evolution of the ⟨1 6 9⟩ orientation single crystals of HSwAl. The experimentally measured texture for the 0% strain (before deformation) is used as the starting texture of the simulations.

⟨1 2 3⟩ orientation, the ⟨1 6 9⟩ orientation still constitutes a different crystallographic orientation. Prediction of its deformation response provides an opportunity to prove the validity of the model (Canadinc et al., 2005) that incorporates the slip system–HDDW interactions into a VPSC algorithm.

Similar to our previous results on the ⟨1 1 1⟩, ⟨0 0 1⟩ and ⟨1 2 3⟩ orientation single crystals of HSwAl (Canadinc et al., 2005), an upward curvature is present in the tensile stress–strain curve of the ⟨1 6 9⟩ orientation. This rapid strain hardening with a coefficient of deformation hardening of $G/41$[2] indicates the significant contribution of the HDDWs to the overall hardening. The corresponding texture evolution (EBSD) is shown on a stereographic triangle in Fig. 6, which clearly indicates the rotation of the initial loading axis (⟨1 6 9⟩ orientation) towards the 1 1 0 pole. Seven texture measurements were taken systematically: prior to deformation, and at strain levels of 0.05, 0.10, 0.20, 0.30, 0.40, and 0.50 (not shown).

Such high coefficients of strain hardening as observed in HSwAl are not prevalent in similar classes of steels that do not display HDDWs, such as the IF-steel (Niendorf et al., submitted for publication) (Fig. 5) and bainitic rail steel (Canadinc et al., 2006), once deformed under tensile loading at similar strain rates. Our recent investigation of monotonic and cyclic response of titanium-stabilized IF steel (Niendorf et al., submitted for publication) revealed that this material responds to tensile loading in a noticeably different way in comparison to HSwAl. A rapid strain hardening leading to an upward stress–strain curve is absent (Fig. 5) for this material.

6. Simulations

Once applied to the HSwAl single crystals of ⟨1 6 9⟩ orientation, the present model successfully predicts the room temperature tensile deformation response (Fig. 5), despite the high-plastic strain levels attained (0.53). The HDDWs were incorporated into the model as explained earlier, however, with one important difference: the orientation information for HDDWs in the ⟨1 6 9⟩ orientation single crystals of HSwAl was not determined experimentally through the conventional trace analysis, although TEM was utilized to prove the existence of HDDWs in this orientation (Fig. 7). As the ⟨1 6 9⟩ orientation is very close to the ⟨1 2 3⟩ orientation, the anisotropic material properties of the two orientations are expected to be similar. Based on this similarity, the experimentally determined spatial orientations of the HDDWs that form in the ⟨1 2 3⟩ orientation single crystals of HSwAl (Canadinc et al., 2005) were utilized in the simulations of the ⟨1 6 9⟩ orientation. The very good agreement between the experimental and simulation results validates this assumption (Fig. 5).

[2] The coefficient of deformation hardening is normalized by the shear modulus (G).

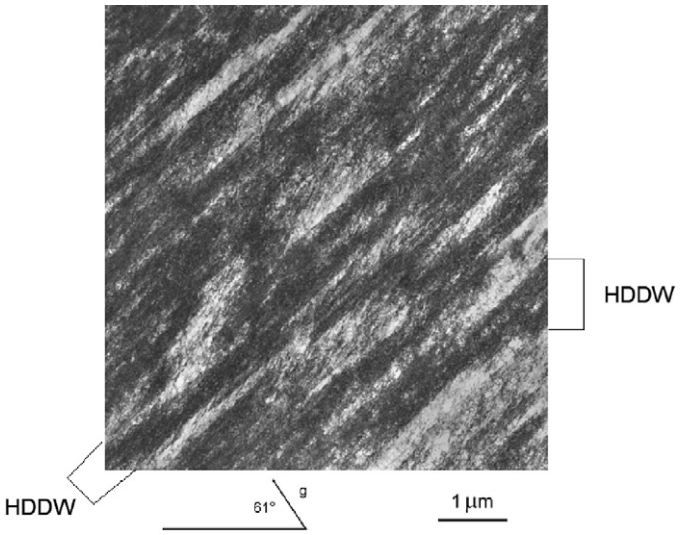

Fig. 7. The microstructure of HSwAl ⟨1 6 9⟩ orientation single crystals at 0.53 plastic strain, displaying HDDWs.

Our previous study on the role of aluminum on the deformation response of Hadfield steel single crystals (Canadinc et al., 2005) showed that twinning was not completely suppressed with the addition of aluminum into the microstructure of Hadfield steel. Although the ⟨1 1 1⟩ and ⟨0 0 1⟩ orientations displayed no twins based on our extensive microstructure analysis, the ⟨1 2 3⟩ orientation exhibited micro-twins (Fig. 8) (Canadinc et al., 2005). Similar to the incorporation of the HDDWs into the present model, we allowed twinning during the deformation of HSwAl ⟨1 6 9⟩ orientation single crystals. The agreement between the experimental and simulation results confirms the approach taken (Fig. 5).

To emphasize the contribution of HDDWs and mechanical twinning to the overall hardening, simulations were run for two other cases: the first case excludes the HDDWs and twins, resulting in a much lower rate of hardening compared to that exhibited by the experimental result (Fig. 5). In the second case, the HDDWs were accounted for, however, the twins were not allowed. The stress levels were much higher than the first hypothetical case of deformation without twins or HDDWs. At high strains, however, stress–strain response simulated without twinning is still substantially lower than the experimental results (Fig. 5). Clearly, the twins

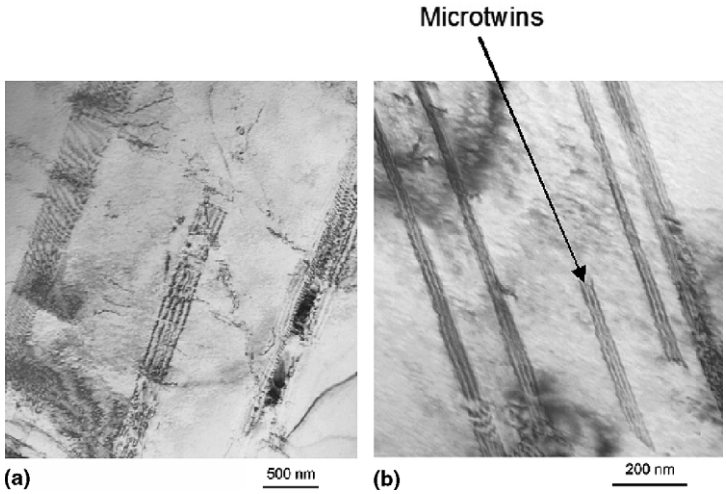

Fig. 8. (a) and (b) HSwAl ⟨1 2 3⟩ orientation subjected to 3% tensile strain. Twins are evident at the early stages of deformation, showing that twinning (micro-twins) was not totally suppressed in the ⟨1 2 3⟩ orientation due to aluminum addition. Although the structures shown in (a) may be mistaken with stacking faults, the contrasts do not fit to stacking faults (Canadinc et al., 2005).

contribute significantly to the overall hardening at plastic strain levels of 0.30 and higher, as twin boundaries act as impenetrable barriers to dislocation motion, similar to the HDDWs.

These observations were useful in determining the role of twinning in the simulations, due to the absence of definitive TEM information about the twin occurrence in the current material. At the initial stages of deformation, twinning was not allowed in the simulations, until the plastic strain level of 0.30. After this point, twinning was allowed to form along with slip.

It is well known that the leading Shockley partial $(1\bar{1}1)[121]$ serves as twinning dislocation, and therefore the corresponding Schmid factors can be considered as Schmid factors for twinning (Karaman, 2000). Accordingly, the Schmid factors for slip and twinning for the $\langle 169\rangle$ orientation under tensile loading are 0.48 and 0.46, respectively. In the VPSC algorithm, the resolved shear stresses of slip and twinning are updated in the same manner (Lebensohn and Tomé, 2002), according to the Voce hardening scheme in the present case. Prior to deformation, the critical resolved shear stress is 159 MPa for slip, and 152 MPa for twinning, and these values correspond to the reference strength values (τ_0) in the Voce hardening scheme (Eqs. (4) and (6)). Nevertheless, twinning is not allowed in the simulations until the plastic strain reaches a value of 0.30. At this point, considering the relationship between the yield strength and critical resolved shear stress through the Schmid's law (Eq. (5)), the critical stress for twinning is 267 MPa. However, at 0.30 plastic strain, the loading direction of the crystal is not $\langle 169\rangle$ any more (Fig. 6), and therefore the Schmid factor 0.46 does not apply. Due to rotation of the tensile axis, the current Schmid factor is 0.43 at 0.30 plastic strain, and the critical stress for twinning is taken as 249 MPa.

Here, we took a simple approach to twinning, and only allowed its inception at the later stages of deformation, based on numerical (this study) and experimental observations (Canadinc et al., 2005). As mentioned previously, the critical stresses for slip and twin initiation are treated similarly. In previous work (Karaman et al., 2000a,b), a model proposed by our group predicted the orientation and stress direction effects on the critical stress for twin initiation. The model incorporated the role of local pile-up stresses, stacking fault energy, the influence of applied stress on the separation of partial dislocations, and the increase in friction stress due to a high-solute concentration. In the current study, we did not take such an approach as the focus is placed on the validation of the recent model that takes into account the HDDWs and their role on the texture evolution. Moreover, the good agreement between the experiments and simulations (Fig. 5) justify the simple approach taken in this study.

The present model was originally developed for three different crystallographic orientations (Canadinc et al., 2005): $\langle 111\rangle$, $\langle 001\rangle$ and $\langle 123\rangle$. Since one of the motivations for undertaking the present study was to extend the use of the model to other crystallographic orientations, the same hardening parameters as in the original study (Canadinc et al., 2005) were utilized in the simulations (Table 1). As explained earlier, the model parameters are determined based on deformation at the slip system level. Thus, the correct model parameters must predict the deformation response of the material, regardless of the crystallographic orientation.

In order to further justify the current model, it is utilized to predict the deformation response of the IF steel (Fig. 5). The model is employed with the same parameters yet some compulsory changes. To begin with, the reference strength (τ_0), which is a material property, is changed to 26 for this polycrystalline body-centered cubic (bcc) steel, as opposed to 159 MPa for HSwAl. This microscopic yield strength value was determined by taking into account the initial texture of the material, its experimentally determined yield strength, and the Taylor factor computed based on the initial texture, following Canadinc et al. (2006). Naturally, the initial texture of the IF steel also differs greatly from that of the single crystalline HSwAl. Specifically, our texture measurements have revealed an initially random texture, yielding a Taylor factor of 3.06. Moreover, the corresponding bcc slip systems ($\langle 111\rangle\{110\}$) were considered in the IF steel simulations, as opposed to $\langle 110\rangle\{111\}$ slip systems in the fcc HSwAl.

Table 1
Numerical values of constants and parameters used in the model (for HSwAl). The units are given in square brackets. ξ, α, and K are dimensionless quantities (Canadinc et al., 2005)

Constant	b [m]	d [m]	ξ	α	K	τ_0 [MPa]
Numerical value	2.58×10^{-10}	6×10^{-7}	0.4	0.4	8×10^{4}	159 (slip); 249 (twinning)

Based on the microstructure investigation carried out on as received IF steel samples (Niendorf et al., submitted for publication), the IF steel does not exhibit HDDWs, and slip dominates the plastic deformation. Therefore, HDDWs and twinning were not allowed in the IF steel simulations, yet the other parameters remained the same as in the HSwAl case. As a result, the model yields a satisfactory prediction of the experimental deformation response for the IF steel (Fig. 5). This further emphasizes the indispensable contribution of HDDWs and twinning to the rapid strain hardening observed in HSwAl.

7. Texture evolution

The texture evolution of the ⟨1 6 9⟩ orientation single crystals of HSwAl was predicted along with the macroscopic deformation response by only considering HDDWs, and by including both HDDWs and twins (Fig. 6). When only HDDWs are accounted for, the model falls short of predicting the texture evolution correctly (Fig. 6). In the second case, where twins are allowed, the texture evolution is predicted with greater success.

Once observed carefully, the twins impose a deviation on the rotation of the loading axis: the rotation still takes place toward the 1 1 0 pole, however, with a deviation toward the 1 2 1 pole. This deviation becomes prevalent at plastic strain levels of 0.30, where the twins are activated in the simulations.

8. Final remarks and discussion

8.1. On the evolution of texture

The studies investigating the texture evolution in materials that exhibit HDDWs have been limited to polycrystals (Winther et al., 1997; Hansen and Juul Jensen, 1992; Juul Jensen and Hansen, 1990; Peeters et al., 2000, 2001). Although the influence of HDDWs on the texture evolution was considered in simulations, these efforts did not go beyond statistical analyses. In the present study, we addressed this issue by predicting the texture evolution in single crystals of HSwAl utilizing a recently proposed model (Canadinc et al., 2005). Specifically, we examined the rotation of the loading axis of HSwAl single crystals due to applied plastic strain.

This study focuses on the texture evolution in single crystals as the rotation of the loading axis of a single crystal constitutes a tractable problem compared to the evolution of texture in a polycrystalline aggregate. In the latter case, the interactions between the neighboring grains and the grain boundary effects make the problem more complicated than it already is.

One noteworthy point regarding the predictions of the texture evolution is that the model yields a smaller rotation of the loading axis, compared to the experimental case (Fig. 6). Even though not drastic, this small difference in the amount of rotation of the loading axis and possible reasons need to be addressed. As explained earlier, the model utilizes the information of wall orientations and presence of twinning from the experimental observations on the ⟨1 2 3⟩ orientation single crystals (Canadinc et al., 2005) to predict the deformation response of the ⟨1 6 9⟩ orientation single crystals of HSwAl. Despite the fact that the tensile deformation response is successfully captured by the model, the determination of wall orientations in the ⟨1 6 9⟩ orientation single crystals through trace analysis might be necessary to achieve perfect predictions of the texture evolution. Another possibility is that the deviation of the prediction of texture evolution from the experimental results might be a result of the dislocation density evolution formulation. In the form given by Eq. (1), the dislocation density evolution strengthens all systems uniformly, such that the self-hardening may be underestimated in the most active slip systems with planes parallel to the HDDWs. Nevertheless, the primary objective of this paper is to extend the use of our microstructure-based model (Canadinc et al., 2005) to various crystallographic orientations. The results (Fig. 6) suggest that the model has the capability to capture the texture evolution along with the macroscopic deformation response under the influence of HDDWs on the matrix.

8.2. Presence and evolution of HDDWs

In this study, we utilized the information regarding the wall orientations from ⟨1 2 3⟩ orientation single crystals of HSwAl in the simulations of the ⟨1 6 9⟩ orientation. Similarly, twinning was also allowed in the

simulations of the ⟨1 6 9⟩ orientation, based on the fact that ⟨1 2 3⟩ and ⟨1 6 9⟩ are very close to each other, suggesting similar material properties for these two orientations.

Once the experimental results (Figs. 5 and 6) are reviewed carefully, the deformation response and texture evolution were predicted with significant success, supporting the aforementioned assumption. It is expected that the conventional trace analysis results regarding the orientation information of HDDWs for ⟨1 2 3⟩ and ⟨1 6 9⟩ orientations coincide. In this work, we wanted to emphasize that utilization of microstructural information about one crystallographic orientation for modeling the deformation response of another orientation that exhibits similar material properties (and degree of anisotropy), without the expense of exhaustive experiments.

8.3. Simulations

Similar to the ⟨1 2 3⟩ orientation case (Canadinc et al., 2005), twins were allowed in the simulations of the ⟨1 6 9⟩ orientation single crystals of HSwAl. Nevertheless, due to lack of experimental data on twinning in the ⟨1 6 9⟩ orientation, especially TEM observations, we do not know at which (exact) strain levels twinning is activated. Ideally, the twinnability and twin initiation stress (Rice, 1992; Tadmor and Bernstein, 2004) should be determined for aluminum alloyed Hadfield steel. However, this is beyond the scope of the study presented herein.

The experimental texture evolution data (Fig. 6) suggests that the initial rotation towards the 1 1 0 pole deviates towards the 1 2 1 pole at plastic strain levels of 0.30. Moreover, results from simulations that did not account for twinning (Fig. 5) show that the experimental deformation response is predicted successfully up to plastic strains levels of only 0.30 in the absence of twins. Accordingly, twinning was allowed in the simulations after 0.30 plastic strain (Fig. 5).

Another important aspect that deserves some discussion is the choice of the modeling approach presented herein. The HDDWs were previously studied with the aid of extended Taylor algorithms that establish the increase in flow stress due to HDDWs (Winther et al., 1997; Hansen and Juul Jensen, 1992; Juul Jensen and Hansen, 1990; Peeters et al., 2000, 2001). Similarly, we chose a crystal plasticity algorithm (VPSC) to model the contribution of HDDWs to the hardening in the single (Canadinc et al., 2005) and polycrystals (Canadinc et al., submitted for publication) of HSwAl. The literature contains examples of similar problems handled by finite element (FE) algorithms. In a previous work (Marketz et al., 2003), α_2 plates in TiAl alloy were modeled as elastic walls that act as a hard second phase and potentially pose barriers against dislocation glide, similar to HDDWs. Nevertheless, the α_2 plates are initially distributed randomly in a FE mesh, and the corresponding volume fraction is constant and does not evolve with deformation, whereas the volume fraction of HDDWs evolve significantly with deformation, and this very important aspect of the problem cannot be accounted for by simply placing elastic walls in a FE mesh. Also, an important distinction we draw between our work and others is that we are comparing textural evolution with precise experimental measurements. Such comparisons have not been attempted in the case of simultaneous twin-HDDW evolution.

Specifically, we incorporate the volume fraction evolution of HDDWs and twins in a VPSC code, and we are able to predict the role of coexisting dense dislocation walls and twins on the macroscopic deformation response. It is possible that these issues can be addressed in a FEM code with extensive modifications in material subroutine codes. But it should be noted that twin reorientation schemes require considerable computational time and our preference is to implement this within the VPSC code.

Other classes of steels that do not display HDDWs, such as the austenitic stainless steels (Karaman et al., 2001a,b,c), Hadfield steels without aluminum (Karaman et al., 2000a,b) and IF steels (Niendorf et al., submitted for publication), do not yield as high coefficients of deformation hardening as the HSwAl, once deformed under tensile loading at similar strain rates. Although this difference in the strain hardening response is attributed to HDDWs, the influence of HDDWs to the deformation response is best illustrated by considering the same material, i.e. HSwAl, with and without HDDWs. The corresponding simulation results shown in Fig. 5 clarify this point and further emphasize the significant influence of HDDWs and the capability of the model to capture this influence on the overall hardening response of the material.

This is accomplished by taking into account the interaction between HDDWs and glide dislocations and the degree of this interaction (Eq. (4)), the rotation and volume fraction evolution of HDDWs), and the fact that HDDWs act as a hard phase in the matrix, similar to precipitates. The HDDWs are incorporated into the VPSC algorithm, such that the trace analysis data defines their orientation in the three dimensional space,

similar to slip and twinning systems. Their rotation and volume fraction evolution due to plastic deformation are accounted through a numerical procedure as adopted in twinning and twinning reorientation schemes. Eliminating the additional terms that modify the classical Voce hardening scheme to yield the expression in Eq. (4) results in a significantly lower strain hardening response for the same material (Fig. 5).

With increasing plastic deformation, both the axis of loading and the HDDWs in the matrix rotate. However, the HDDWs are not fixed to the lattice, thus the rotation of HDDWs takes place independent of that of the loading axis, or in other words, HDDWs rotate (or spin) independent of the lattice itself. In order to account for this feature, the numerical procedure utilized in twin reorientation is adopted in the current model (Canadinc et al., 2005). Moreover, the independent rotation of HDDWs implies that the dislocations that make up the HDDWs move, as well, but their motion is limited to the incremental spin due to plastic deformation. This phenomenon brings about the continuous change in the HDDW–slip system interactions, which is accounted for in the current model.

In a recent work (Canadinc et al., submitted for publication), we studied the polycrystalline response of the HSwAl in the presence of HDDWs, utilizing a novel approach, such that the trace analysis results of the $\langle 1\,1\,1\rangle$ orientation single crystals were utilized to represent the HDDWs in polycrystals. Successful application of the model to polycrystals is now further supported by the validation of the model through its application to a different crystallographic orientation and monitoring of the corresponding texture evolution. This provides a venue for its application to other materials and alloys that display HDDWs or similar crystallographic features.

The success of the model in predicting the deformation response of materials that do not exhibit HDDWs is also of great importance since this would serve as emphasizing the contribution of HDDWs to the hardening by showing that the current model is not material specific. With this motivation, utilizing the same parameters, the deformation response of the titanium-free IF steel, which does not exhibit HDDWs, was simulated. The satisfactory prediction of the stress–strain curve shows that a rapid strain hardening is not present in the absence of HDDWs.

9. Conclusions

The tensile deformation response and the corresponding texture evolution in the $\langle 1\,6\,9\rangle$ oriented single crystals of aluminum alloyed Hadfield steel (HSwAl) were studied. A recently proposed (Canadinc et al., 2005) visco-plastic self-consistent (VPSC) model was utilized in the simulations. The following conclusions are drawn from the work presented herein:

1. The macroscopic tensile deformation response of the $\langle 1\,6\,9\rangle$ orientation single crystals of HSwAl was successfully predicted utilizing the microstructure-based model. We note that the model is indeed 'predictive' because it proved successful in single crystal orientations other than that used to establish the hardening parameters and constants.
2. The model was utilized to predict the rotation of the loading axis of the $\langle 1\,6\,9\rangle$ orientation single crystals of HSwAl due to applied plastic strain taking into account the high-density dislocation walls (HDDWs). The results suggest that the model is capable of predicting the texture evolution in single crystals in the presence of HDDWs in the matrix.
3. The wall orientation observations and hardening parameters for the $\langle 1\,2\,3\rangle$ orientation single crystals were utilized in the simulations of the $\langle 1\,6\,9\rangle$ orientation. The good agreement between the experiments and simulations promote the use of microstructural information of one orientation for the simulations of another that has similar material properties.
4. The results encourage the utilization of the model for predicting the deformation response and texture evolution of other orientations of HSwAl. Eventually, the utilization of the model could be extended to polycrystals of HSwAl and other alloys that exhibit HDDWs.

Acknowledgements

This work was supported by the National Science Foundation grant DMR-0313489. The authors are grateful to Dr. Armand J. Beaudoin for his suggestions.

References

Adler, P.H., Olson, G.B., Owen, W.S., 1986. Met. Trans. A 17, 1725.
Brown, L.M., Clarke, D.R., 1975. Acta Metall. 23, 821.
Bunge, H.J., 1969. Mathematische Methoden der Texturanalyse. Akademie-Verlag, Berlin.
Canadinc, D., Karaman, I., Sehitoglu, H., Chumlyakov, Y.I., Maier, H.J., 2003. Metall. Mater. Trans. A 34, 1821.
Canadinc, D., Sehitoglu, H., Maier, H.J., Chumlyakov, Y.I., 2005. Acta Mater. 53, 1831.
Canadinc, D., Sehitoglu, H., Maier, H.J., 2006. Unpublished work.
Canadinc, D., Sehitoglu, H., Maier, H.J., submitted for publication. Mater. Sci. Eng. A.
Dastur, Y.N., Leslie, W.C., 1981. Met. Trans. A 12, 749.
Hansen, N., Juul Jensen, D., 1992. Acta Metall. Mater. 40, 3265.
Hosford, W.F., 1993. The Mechanics of Crystals and Textured Polycrystals. Oxford University Press, New York.
Hull, D., Bacon, D.J., 2002. Introduction to Dislocations. Butterworth-Heinemann, Oxford.
Juul Jensen, D., Hansen, N., 1990. Acta Metall. Mater. 38, 1369.
Karaman, I., 2000. PhD Thesis, University of Illinois at Urbana-Champaign, USA.
Karaman, I., Sehitoglu, H., Gall, K., Chumlyakov, Y.I., Maier, H.J., 2000a. Acta Mater. 48, 1345.
Karaman, I., Sehitoglu, H., Beaudoin, A.J., Chumlyakov, Y.I., Maier, H.J., Tomé, C.N., 2000b. Acta Mater. 48, 2031.
Karaman, I., Sehitoglu, H., Chumlyakov, Y.I., Maier, H.J., Kireeva, I.V., 2001a. Metall. Mater. Trans. A 32, 695.
Karaman, I., Sehitoglu, H., Maier, H.J., Chumlyakov, Y.I., 2001b. Acta Mater. 49, 3919.
Karaman, I., Sehitoglu, H., Chumlyakov, Y.I., Maier, H.J., Kireeva, I.V., 2001c. Scripta. Mater. 44, 337.
Kocks, U.F., Tomé, C.N., Wenk, H.R., 2000. Texture and Anisotropy, second ed. Cambridge University Press.
Lebensohn, R.A., Tomé, C.N., 1993. Acta Metall. Mater. 41, 2611.
Lebensohn, R.A., Tomé, C.N., 2002. Manual for Code Visco-Plastic Self-Consistent Version 5.
Liu, Q., Hansen, N., 1995. Phys. Status Solidi A 149, 187.
Liu, Q., Juul Jensen, D., Hansen, N., 1998. Acta Mater. 46, 5819.
Marketz, W.T., Fischer, F.D., Clemens, H., 2003. Int. J. Plast. 19, 281.
Niendorf, T., Canadinc, D., Maier, H.J., Karaman, I., Sutter, S.G., submitted for publication. Z. Metallkde.
Owen, W.S., Grujicic, M., 1999. Acta Mater. 47, 111.
Peeters, B., Kalidindi, S.R., Van Houtte, P., Aernoudt, E., 2000. Acta Mater. 48, 2123.
Peeters, B., Seefeldt, M., Teodosiu, C., Kalidindi, S.R., Van Houtte, P., Aernoudt, E., 2001. Acta Mater. 49, 1607.
Raghavan, K.S., Sastri, A.S., Marcinkowski, M.J., 1969. Trans. TMS-AIME 245, 1569.
Raphanel, J.L., Schmitt, J.H., Baudelet, B., 1992. In: Proceedings of the 8th Risø International Symposium on Materials Science, Denmark, p. 491.
Rice, J.R., 1992. J. Mech. Phys. Solids 40, 239.
Saada, G., 1960. Acta Metall. 8, 841.
Shtremel, M.A., Kovalenko, I.A., 1987. Phys. Met. Metall. 63, 158.
Tadmor, E.B., Bernstein, N., 2004. J. Mech. Phys. Solids 52, 2507.
Turner, P.A., Tomé, C.N., Christodoulou, N., Woo, C.H., 1999. Philos. Mag. A 79, 2505.
Venables, J.A., 1963. J. Phys. Chem. Solids 25, 693.
Weertman, J., Weertman, J.R., 1992. Elementary Dislocation Theory. Oxford University Press, New York.
Winther, G., 1998. In: Proceedings of the 19th Risø International Symposium on Materials Science, Denmark, p. 185.
Winther, G., Juul Jensen, D., Hansen, N., 1997. Acta Mater. 45, 5059.
Zakharova, E.G., Kireeva, I.V., Chumlyakov, Y.I., Efimenko, S.P., Sehitoglu, H., Karaman, I., 2002. Doklady Phys. 47, 515.